Monoclonal Antibody-Light chain CDR1/Spike Glycoprotein Receptor Binding Domain Dissociation Explains Antibody Escape Mechanism in L452R-SARS-CoV-2

olaposi omotuyi[1], Oyekanmi Nash[2], babatunji Oyinloye[3], Mustapha Popoola[4], Ayodele Ajayi[3], and Victor UKwenya[5]

[1]Adekunle Ajasin University
[2]National Biotechnology Development Agency
[3]Afe Babalola University
[4]Tertiary Education Trust Fund
[5]Federal University of Technology Akure

March 07, 2024

Abstract

Most of the well-characterized innate antibodies elicited by exposure to SARS-CoV-2 or a vaccine targets the spike glycoprotein receptor-binding domain (RDB) which doubles as the angiotensin-converting enzyme 2 (ACE2, receptor) binding. RBD mutation is therefore a potential health concern in COVID-19 pandemic. RBD-L452R-SARS-CoV-2 exhibits increased transmissibility and immune evasion with an unknown underlying mechanisms. The immune evasion mechanism was investigated here. in R452, loss of hydrophobic interaction between RBD-L452/HCDR3-I103 disrupts RBD-E484/heavy-chain-R112 salt-bridge, and cation-π interaction between RBD-E484/mAB-Y32(LcCDR1). Unburied RBD flips ˜64° from the antibody plane, losing all interaction with the mAB light chain-CDR; thus, making ternary complex thermodynamically unstable.

Monoclonal Antibody-Light chain CDR1/Spike Glycoprotein Receptor Binding Domain Dissociation Explains Antibody Escape Mechanism in L452R-SARS-CoV-2

Abstract:

Omotuyi, I. Olaposi[1,2,3], Nash Oyekami[4], Oyinloye, B. Emmanuel[1,2], Popoola, M. Ayodele[1,6], Ajayi, A. Ebenezer[1,5], and UKwenya, V.[7]

[1]Center for Drug Research and Development, Afe Babalola University, Ado-Ekiti, Ekiti State, Nigeria.
[2]Cheminformatics and Simulation Unit, Mols & Sims, Ado-Ekiti, Ekiti State, Nigeria.
[3]Department of Biochemistry, Adekunle Ajasin University, Ondo State, Nigeria.
[4]Center for Genomics Research and Innovation, National Biotechnology Development Agency, Abuja, Nigeria.
[5]Institut fur pflanzenernahrung und Bodenkunde, Christian-Albrechts Universitat zu Keil, Hermann Rodewaldstr. 2, 24118 Kiel. Germany.
[6]Research and Development Desk, Office of the Executive Secretary, Tertiary Education Trust Fund, Abuja, Nigeria.
[7]Department of Human Anatomy, School of Health and Health Technology, Federal University of Technology, Akure, Ondo State, Nigeria

Abstract

Most of the well-characterized innate antibodies elicited by exposure to SARS-CoV-2 or a vaccine targets the spike glycoprotein receptor-binding domain (RDB) which doubles as the angiotensin-converting enzyme 2 (ACE2, receptor) binding. RBD mutation is therefore a potential health concern in COVID-19 pandemic.

RBD-L452R-SARS-CoV-2 exhibits increased transmissibility and immune evasion with an unknown underlying mechanisms. The immune evasion mechanism was investigated here.

in R452, loss of hydrophobic interaction between RBD-L452/HCDR3-I103 disrupts RBD-E484/heavy-chain-R112 salt-bridge, and cation-π interaction between RBD-E484/mAB-Y32(LcCDR1).

Unburied RBD flips ~64° from the antibody plane, losing all interaction with the mAB light chain-CDR; thus, making ternary complex thermodynamically unstable.

Keywords: L-452R-SARS-CoV-2, spike glycoprotein, Immune evasion mechanism,

INTRODUCTION

SARS-CoV-2 has now infected more than 157 million and caused the death of approximately 3.3 million people globally in three fast-successive waves [1]. The hope of humanity now squarely lies in the collective ability of scientists to develop curative or prophylactic agents such as therapeutics and vaccines. Currently, there are about five major vaccines available for clinical use against COVID-19, these are: Ad26.COV2.S (*Johnson&Johnson*), ChAdOx1-S (Oxford-Uni/AstraZeneca), BNT162b2 (*Mordena, Pfizer-BioNtech*), Sputnik V (*Gamaleya Research Institute of Epidemiology and Microbiology*) and the CoronaVac (*Sinovac Biotech*) [2] but therapeutics have not been very successful clinically.

The recent surge in SARS-CoV-2 mutations, especially around the vaccine-targeted spike glycoprotein receptor-binding domain (RBD) epitopes has begun to heighten concerns about the fate of current vaccines given their mechanistic nature [3]. Predominant among the RBD mutations causing concerns are D614G; found in SARS-CoV-2 variants B.1.1.7 (UK) and B.1.351 (South Africa) [4, 5] and the more recent L452R (B.1.429) and E484Q (B.1.351); circulating in Indian population [6].

Whilst L452R and E484Q mutations have been shown to demonstrate capacity for immune evasion [6, 7], the underlying mechanisms have not been studied. The current study therefore sought to understand the atomistic basis for immune evasion in L452R RBD mutation.

To this end, the 3D structure of a neutralizing antibody (P2B-2F6 Fab type; hereafter referred to as mAB) specifically elicited by SARS-CoV-2 spike glycoprotein RBD and bearing no cross-neutralization with SARS-CoV-RBD or MERS-CoV-RBD [8] was used. Two complexes were generated for the experiments; the wildtype (WT) and the L452R-RBD mutant (MT) in mAB-bound states.

METHODS

The wildtype structure used for this study is a re-modelled structure of SARS-CoV-2 antibody bound to RBD based on the x-ray crystal structure deposited by Ju *et al*. (PDB ID: 7BWJ)[8]. The L452R-SARS-CoV-2-RBD mutant structure was generated using mutagenesis plugin in PyMol [9]. All residues in both complexes were protonated at p^H 7.4 and prepared for Molecular Dynamics (MD) simulation using CHARMM-GUI platform [10]. All proteins residues were parameterized using CHARMM36 forcefield and fully immersed in an octahedral box of TIP3P water model [11] and neutralized using Na^+/Cl^-. All simulations were performed using periodic boundary conditions (PBC), all long range electrostatic interactions were calculated using Ewald summation [12] while the SHAKE algorithm was used to fix hydrogen bonds. Integration of atomic motions (2 fs time step) was done using Newtonian equations, while the Berendsen thermostat and barostat algorithms were used in temperature and pressure controls respectively [13].

The Biosystems were fully equilibrated following 20 ns NVT ensemble (at 300 K), and 30 ns density equilibration (NPT ensemble) with full restraints on the heavy atoms of the protein. Production MD runs was terminated after 110 ns with data collection every 250 ps for QC and analysis.

All 3D representation was generated using PyMol [9], slat-bridge analysis was performed using salt-bridge plugin, while distance analysis was performed using PLUMED plugin in visual molecular dynamics (VMD) software [14]. Population distribution of distance was plotted using GraphPad Prism (*ver*. 9) while MATHEMATICA was used to generate the 3D free energy landscapes using in house scripts [15]. Network analysis was also performed using Network-Tools in VMD.

RESULTS AND DISCUSSION

Following 110 ns production simulation, the Cα-Cα distance around three paratope (Y27-heavy chain Complementarity-determining region 1 (CDR1), I103-HCDR3 and Y32-Light chain CDR1) and RBD residues (G446 (around HCDR1-Y27), L/R-452 (around I103-HCDR3) and (V483-around Y32-Light chain CDR1) were monitored (Fig. 1A) to assess the initial binding events of the complexes. RBD-G446 in both the wildtype and mutant complexes stayed fully bound (≈ 9.0 Å) to the mAB-HCDR1-Y27 after 70 ns despite the initial unbinding events earlier in the simulation (MT (15-25 ns), WT (45-60 ns)) Fig.1B, *i*). The population distribution of Cα-Cα distance between mAB-I103-HCDR3 and RBD-L/R452 strongly indicated that the mutant preferentially sampled unbound states (NB > 10. 0 Å) whereas the wildtype samples flexibly between partially-(PB) and fully-bound states (FB) and very rarely NB state (Fig.1B, *ii*). The data further revealed that unbinding events progressed with the simulation (data not shown) as indicated for the inter-atomic distances sampled in the last 20 ns in both complexes (inset). In MT complex, RBD-V483 completely dissociated from mAB-Y32-Light chain CDR1starting from ≈ 65 ns (> 10.0 Å) and did not recover for the rest of the simulation whist the residues stayed fully bound in the WT complex (Fig.1B, *iii*). These data provide initial indication that stable binding event at L-452/I103 may play important role in stabilizing RBD-mAB-light chain interaction but this is very serendipitous as there is RBD-E484 which exists in optimal salt-bridge interaction distance from heavy chain-R112 (Fig.1C, *i*). Although, E484Q mutation is also associated with antibody escape [6]. RBD-E484-mAB-112 failed to stabilize the complex as the salt-bridge was completely broken (> 8.0 Å) starting from around 70 ns (Fig.1C, *ii*). These data strongly indicate that L-452 forms very key hydrophobic interaction with mAB-I103 and possibly V105, V106 and P107 which are all located within the HCDR3; this interaction provides the necessary pull to stabilize RBD-E484-mAB-112 salt-bridge interaction. Guanidinium cap of R452 is thought to disrupt this interaction causing loss of interaction to mAB-light chain.

In order to validate that the interaction between RBD and light-chain mAB was lost in L452R-RBD-mAB complex, network analysis was conducted on conformations sampled within the last 70 ns of the simulation and distilled into the critical nodes. The data showed that RBD-N450/mAB-H54(HCDR2), RBD-Y449/mAB-Y33(HCDR1), RBD-F490/mAB-V106(HCDR3), RBD-E484/mAB-Y32(LcCDR1) are critical pairs stabilizing the complex in the wildtype (Fig. 1D, *i*) and all but RBD-Y449/mAB-Y33(HCDR1) and D-F490/mAB-V105(HCDR3) were lost in L452R mutant (Fig. 1D, *ii*) lending credence to the loss of light chain CDR1 interaction.

Lastly, the center of mass distance (COM) between Cα-RBD and mAB and Cα-rmsd from PDB ID: 7bwj [8] were projected along the Free Energy Landscape (FEL) in order to evaluate representative structures sampled in the conformational basins (Fig. 2). A general first observation is that COM for both complexes were within

50.0 ~56.0 Å, indicating that complete dissociation of the ternary complex did not occur. The MT structures were largely sampled around 4.0-6.0 Å Cα-rmsd from PDB ID: 7bwj whilst the WT sampled thermodynamically stable conformations around 2-4 Å (Fig. 2, A&B) which strongly points to re-arrangement of the ternary complex in MT. Three MT complexes were retrieved from the conformational basins (Fig. 2A, *i-iii*), these results showed that thermodynamically, instability is initiated by increase in RBD-mAB/light chain distance (Fig. 2A, *i-ii*) and fully committed when this event couples with flipping of the RBD to ~64° from the initial plane (Fig. 2A, *iii*). WT complex does sample transient RBD-light chain dissociation (Fig. 2B, *i*) but this is not associated with the flipping event, therefore, allowing the samples to re-sample very stable ternary conformation (Fig. 2B, *ii*).

Our data have provided significant insight into the underlying mechanism for immune evasion in L452R-SARS-CoV-2; in furtherance to this, a recent publication [16] identified this mutation as proximal to the furin cleavage site with capacity to improve ACE2 recognition and binding; thus resulting in increased transmissibility. Increased transmissibility coupled with decreased mAB and neutralization are recipe for public health situation. Additionally, whether the current RBD-targeting vaccines [17-19] will elicit necessary immunobiology to neutralize L452R-SAR-CoV-2 strains is already experimentally doubtful [20] and may therefore require immediate field-level investigation.

ACKNOWLEDGMENTS
The authors would like to acknowledge funding from Adekunle Ajasin University, Akungba-Akoko Biomedical Research grant (grant no: ADV/50/2016/000004) H3-Africa Bio-informatics Network: (to Prof. Nash Oyekanmi) (NIH Common Fund Award/NHGRI Grant grant no: U41HG006941). None of the authors declare conflict of interest

Legend of figures:

Figure 1.0: L452R-SARS-CoV-2-RBD mutation perturb key interactions required for mAB binding. (A) Cartoon representation of RBD (gray) and mAB (blue/green) showing key amino acids (spheres) at the binding interface. (B, *i*) Line graph representing mean distance between G446 (RBD) and Y27 (mAB) during MD simulation. (ii) population distribution of Cα-Cα distance between residue 452 (RBD) and I103 (mAB) (*iii*) Line graph representing mean distance between V483 (RBD) and Y32 (mAB) during MD simulation. (C, *i*). 3D cartoon representation of the spatial position of E484 (RBD) and R112 (mAB) indicating a potential salt-bridge. (ii), Line graph representing mean distance E484 (RBD) and R112 (mAB) during MD simulation. (D) Network analysis showing communication between RBD and mAB in wildtype (i) and mutant (ii) complexes.

Figure 2.0: L452R-SARS-CoV-2-RBD mutation alter the Free Energy Landscape (FEL) when interacting with mAB . (A) FEL of the L452R-SARS-CoV-2-RBD/mAB complex projected along center of mass (COM) distance (between RBD and mAB) and root mean square distance from PDB ID: 7bwj. (B) FEL of the R452-SARS-CoV-2-RBD/mAB complex projected along center of mass (COM) distance (between RBD and mAB) and root mean square distance from PDB ID: 7bwj. The 3D structures of the representative coordinates are represented as *"i", "ii" and "iii"* respectively.

References:

1 Adil MT, Rahman R, Whitelaw D, Jain V, Al-Taan O, Rashid F, Munasinghe A*, et al.* SARS-CoV-2 and the pandemic of COVID-19. Postgrad Med J 2021, 97: 110-116

2 Hodgson SH, Mansatta K, Mallett G, Harris V, Emary KRW, Pollard AJ. What defines an efficacious COVID-19 vaccine? A review of the challenges assessing the clinical efficacy of vaccines against SARS-CoV-2. Lancet Infect Dis 2021, 21: e26-e35

3 Greaney AJ, Starr TN, Gilchuk P, Zost SJ, Binshtein E, Loes AN, Hilton SK*, et al.* Complete Mapping of Mutations to the SARS-CoV-2 Spike Receptor-Binding Domain that Escape Antibody Recognition. Cell Host Microbe 2021, 29: 44-57 e49

4 Omotuyi IO, Nash O, Ajiboye OB, Iwegbulam CG, Oyinloye EB, Oyedeji OA, Kashim ZA*, et al.* Atomistic simulation reveals structural mechanisms underlying D614G spike glycoprotein-enhanced fitness in SARS-COV-2. J Comput Chem 2020, 41: 2158-2161

5 Ho D, Wang P, Liu L, Iketani S, Luo Y, Guo Y, Wang M*, et al.* Increased Resistance of SARS-CoV-2 Variants B.1.351 and B.1.1.7 to Antibody Neutralization. Res Sq 2021,

6 McCallum M, Bassi J, Marco A, Chen A, Walls AC, Iulio JD, Tortorici MA*, et al.* SARS-CoV-2 immune evasion by variant B.1.427/B.1.429. bioRxiv 2021,

7 Deng X, Garcia-Knight MA, Khalid MM, Servellita V, Wang C, Morris MK, Sotomayor-Gonzalez A*, et al.* Transmission, infectivity, and antibody neutralization of an emerging SARS-CoV-2 variant in California carrying a L452R spike protein mutation. medRxiv 2021,

8 Ju B, Zhang Q, Ge J, Wang R, Sun J, Ge X, Yu J*, et al.* Human neutralizing antibodies elicited by SARS-CoV-2 infection. Nature 2020, 584: 115-119

9 Mooers BHM, Brown ME. Templates for writing PyMOL scripts. Protein Sci 2021, 30: 262-269

10 Choi YK, Park SJ, Park S, Kim S, Kern NR, Lee J, Im W. CHARMM-GUI Polymer Builder for Modeling and Simulation of Synthetic Polymers. J Chem Theory Comput 2021, 17: 2431-2443

11 Boonstra S, Onck PR, Giessen E. CHARMM TIP3P Water Model Suppresses Peptide Folding by Solvating the Unfolded State. J Phys Chem B 2016, 120: 3692-3698

12 Wells BA, Chaffee AL. Ewald Summation for Molecular Simulations. J Chem Theory Comput 2015, 11: 3684-3695

13 Fuzo CA, Degreve L. Effect of the thermostat in the molecular dynamics simulation on the folding of the model protein chignolin. J Mol Model 2012, 18: 2785-2794

14 Humphrey W, Dalke A, Schulten K. VMD: visual molecular dynamics. J Mol Graph 1996, 14: 33-38, 27-38

15 Omotuyi OI, Nagai J, Ueda H. Lys39-Lysophosphatidate Carbonyl Oxygen Interaction Locks LPA1 N-terminal Cap to the Orthosteric Site and partners Arg124 During Receptor Activation. Sci Rep 2015, 5: 13343

16 Cherian S, Potdar V, Jadhav S, Yadav P, Gupta N, Das M, Das S*, et al.* Convergent evolution of SARS-CoV-2 spike mutations, L452R, E484Q and P681R, in the second wave of COVID-19 in Maharashtra, India. bioRxiv 2021: 2021.2004.2022.440932

17 Ewer KJ, Barrett JR, Belij-Rammerstorfer S, Sharpe H, Makinson R, Morter R, Flaxman A*, et al.* T cell and antibody responses induced by a single dose of ChAdOx1 nCoV-19 (AZD1222) vaccine in a phase 1/2 clinical trial. Nat Med 2021, 27: 270-278

18 Stephenson KE, Le Gars M, Sadoff J, de Groot AM, Heerwegh D, Truyers C, Atyeo C*, et al.* Immunogenicity of the Ad26.COV2.S Vaccine for COVID-19. JAMA 2021, 325: 1535-1544

19 Ebinger JE, Fert-Bober J, Printsev I, Wu M, Sun N, Prostko JC, Frias EC*, et al.* Antibody responses to the BNT162b2 mRNA vaccine in individuals previously infected with SARS-CoV-2. Nat Med 2021,

20 Starr TN, Greaney AJ, Dingens AS, Bloom JD. Complete map of SARS-CoV-2 RBD mutations that escape the monoclonal antibody LY-CoV555 and its cocktail with LY-CoV016. Cell Rep Med 2021, 2: 100255

1A

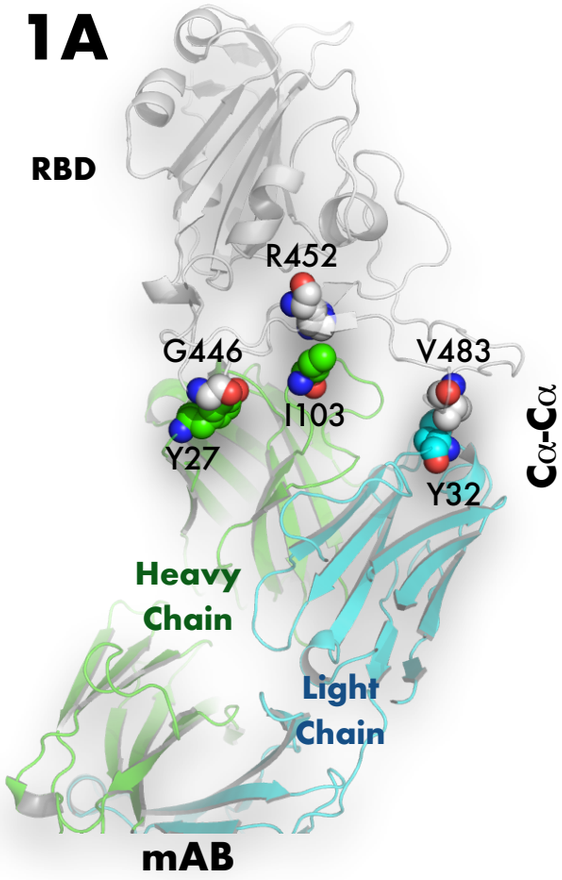
RBD
R452
G446
V483
I103
Y27
Y32
Heavy Chain
Light Chain
mAB

1B

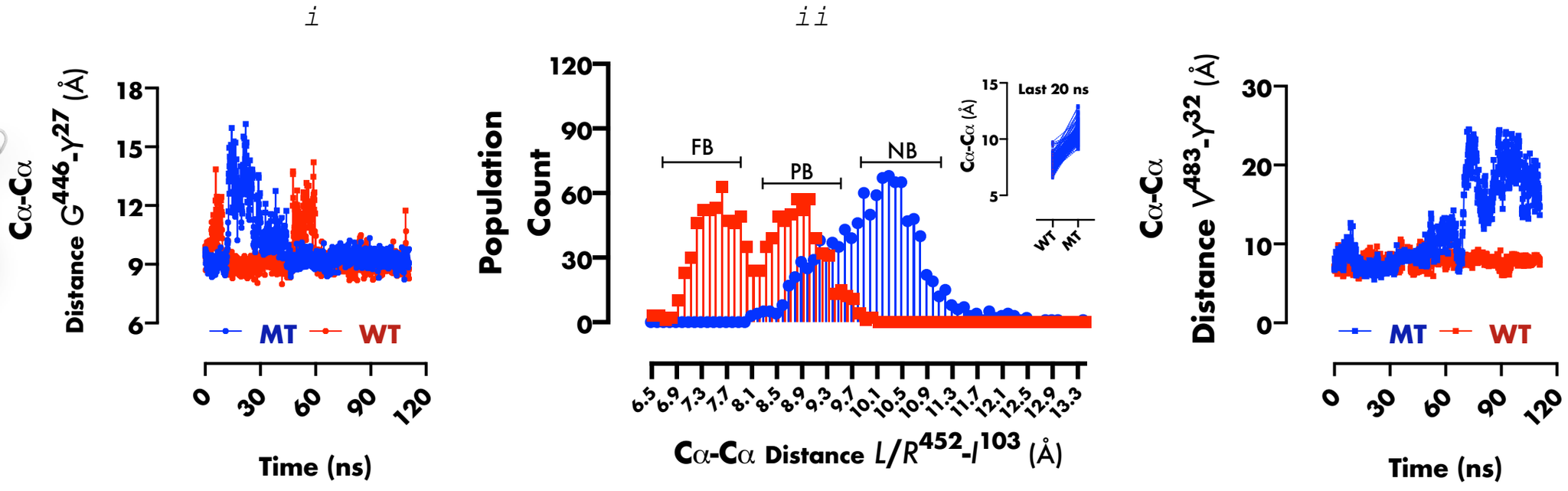
i
ii
iii
Cα-Cα Distance G446-Y27 (Å)
MT
WT
Time (ns)
Population Count
FB
PB
NB
Last 20 ns
Cα-Cα (Å)
WT
MT
Cα-Cα Distance L/R452-I103 (Å)
Cα-Cα Distance V483-Y32 (Å)

1C

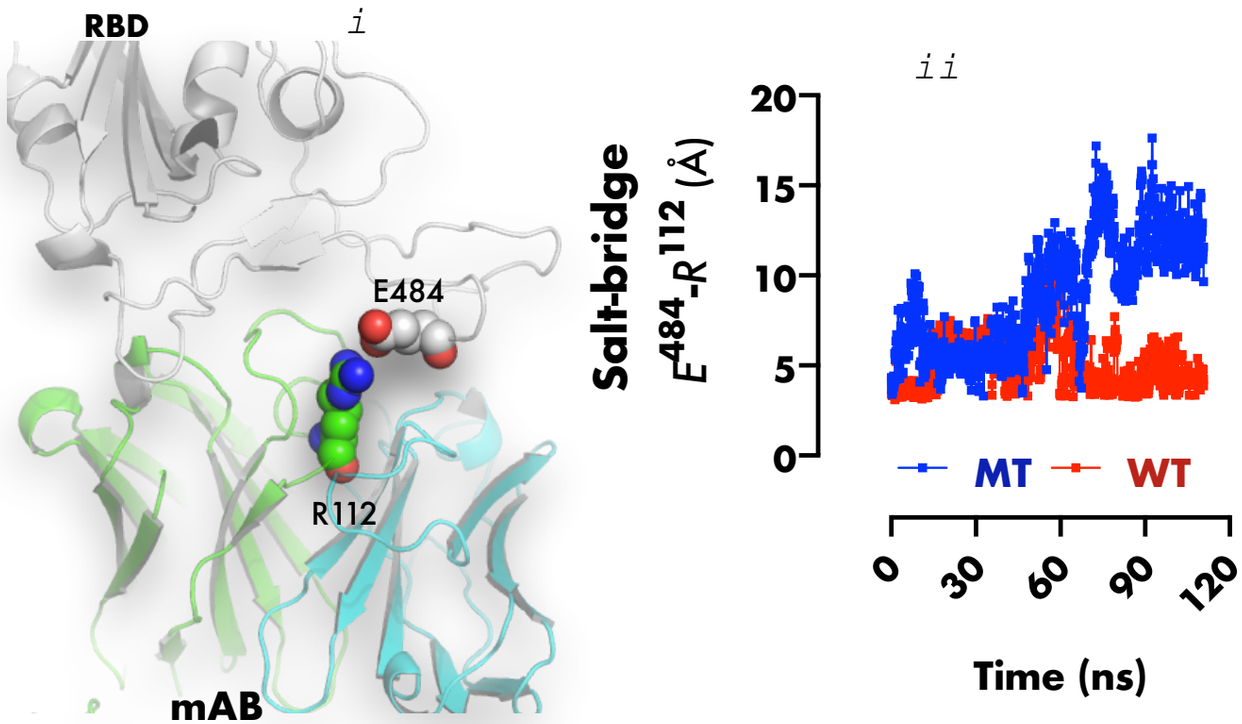
RBD
i
E484
R112
mAB
ii
Salt-bridge E484-R112 (Å)
MT
WT
Time (ns)

1D

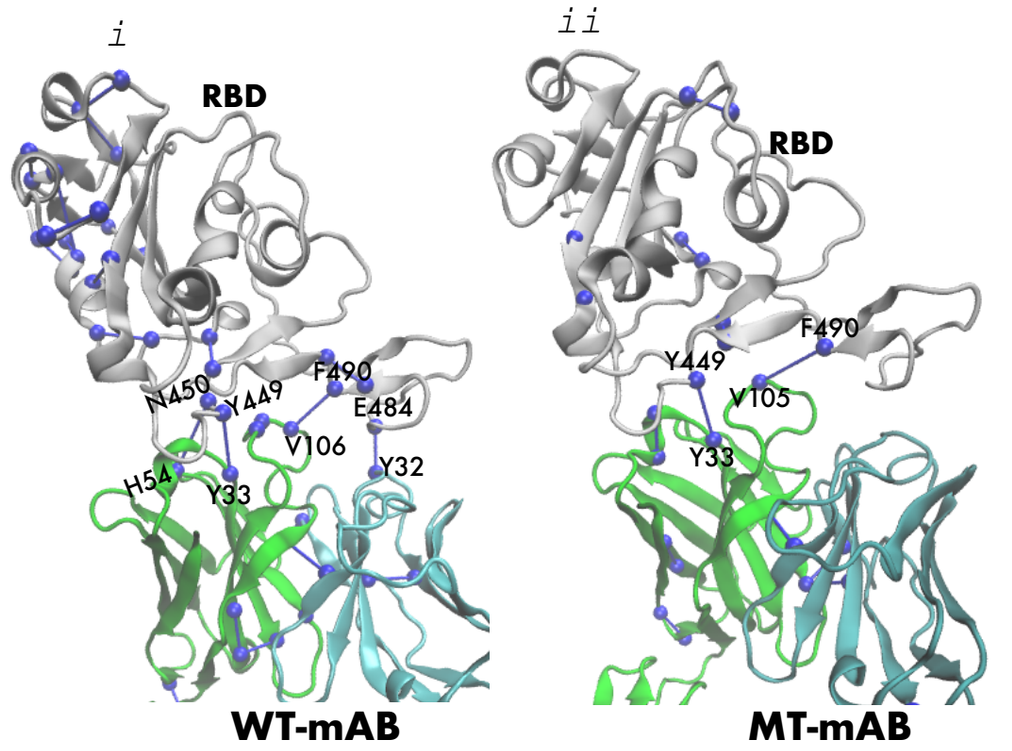
i
ii
RBD
RBD
N450
Y449
F490
E484
V106
Y32
H54
Y33
Y449
F490
V105
Y33
WT-mAB
MT-mAB

2

A

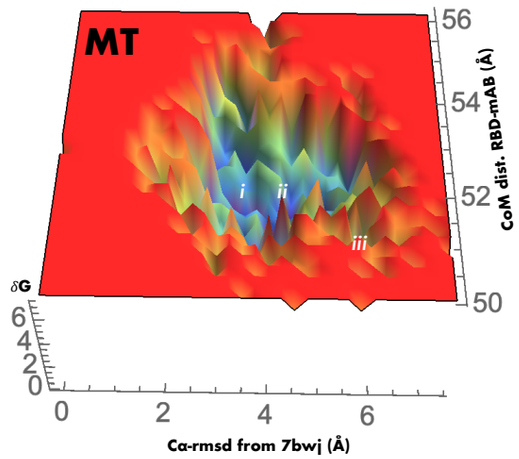
MT
i
ii
iii
δG
6
4
2
0
0
2
4
6
Cα-rmsd from 7bwj (Å)
56
54
52
50
CoM dist. RBD-mAB (Å)

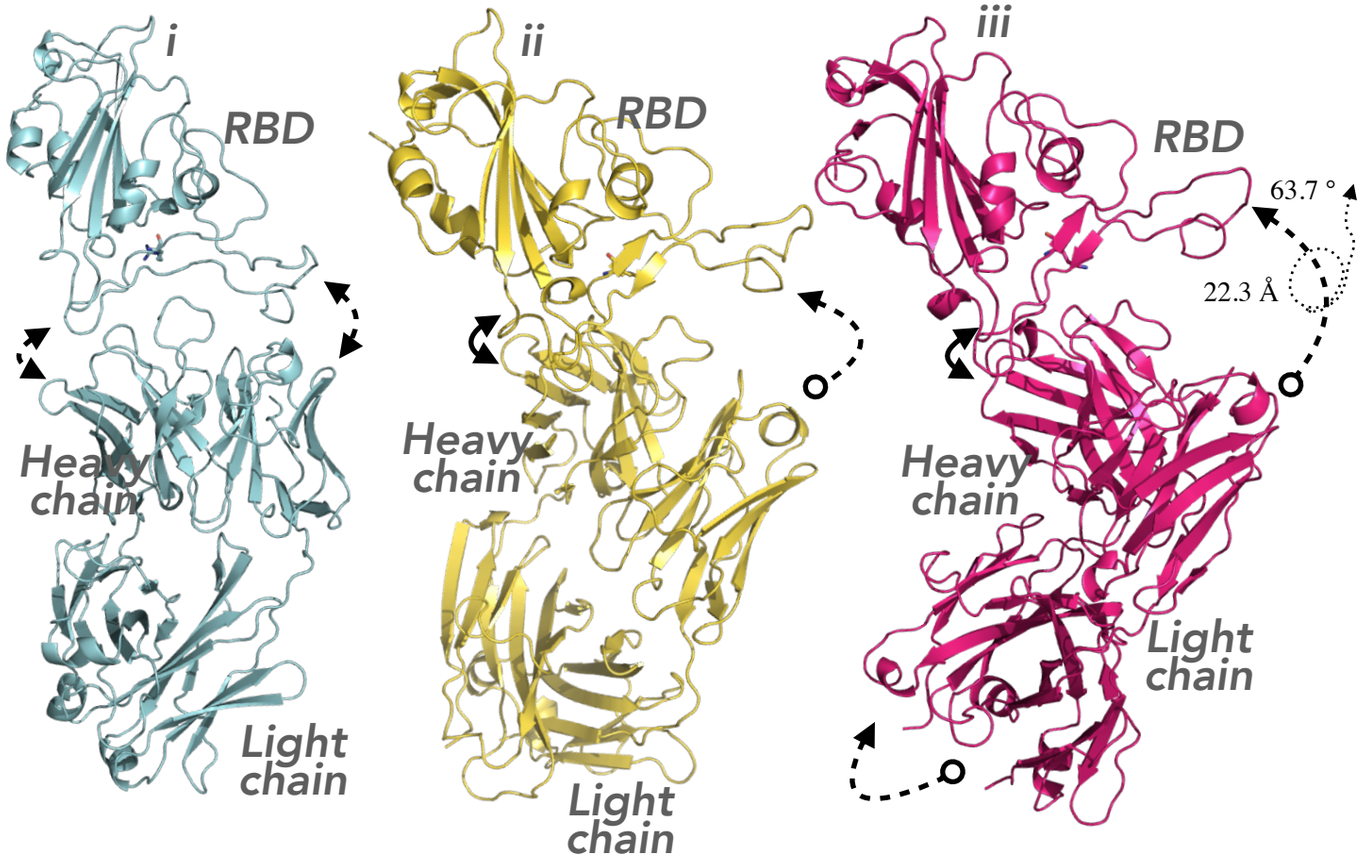
i
RBD
Heavy chain
Light chain
ii
RBD
Heavy chain
Light chain
iii
RBD
63.7 °
22.3 Å
Heavy chain
Light chain

B

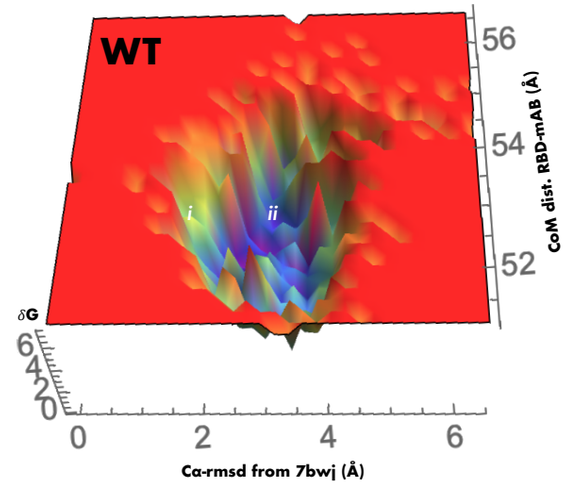
WT
i
ii
δG
6
4
2
0
0
2
4
6
Cα-rmsd from 7bwj (Å)
56
54
52
CoM dist. RBD-mAB (Å)

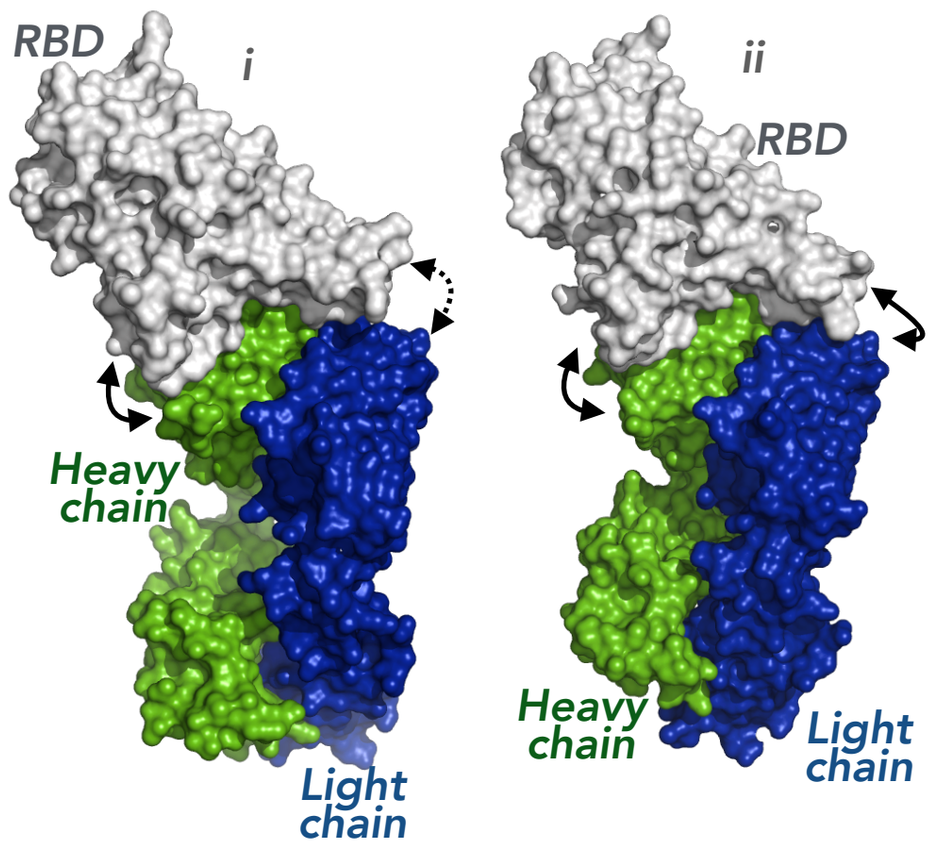
RBD
i
Heavy chain
Light chain
ii
RBD
Heavy chain
Light chain